NMR Investigations of In-Situ Stretched Block Copolymers of Poly(butylene terephthalate) and Poly(tetramethylene oxide)

Angelika Schmidt and Wiebren S. Veeman*

Physikalische Chemie, Gerhard-Mercator-Universität-Duisburg, Lotharstrasse 1, 47057 Duisburg, Germany

Victor M. Litvinov and Wouter Gabriëlse

DSM Research B.V., PAC-MC, P.O. Box 18, 6160 MD Geleen, The Netherlands

Received October 7, 1997; Revised Manuscript Received December 20, 1997

ABSTRACT: The changes in phase structure under mechanical deformation of poly(butylene terephthalate) (PBT)/poly(tetramethylene oxide) (PTMO) multiblock copolymers differing in the amount and block length of PTMO have been investigated by ^{13}C magic-angle-spinning NMR. Measurements have been performed on *unstretched* samples, on *stretched* samples allowed to relax before the NMR experiment, and on samples that are kept under tension in the spinning rotor (*in-situ stretched*). For *unstretched* samples a heterogeneity in NMR relaxation behavior of the OCH_2 carbons of PTMO was observed (T_{CH}, $^{13}C-T_{1\rho}$, $^{1}H-T_{1\rho}$), which is attributed to a microphase separation in the amorphous phase into a PTMO-rich phase (mobile) and a mixed PBT/PTMO phase (restricted mobility). Long PTMO block lengths and high PTMO contents favor the formation of the PTMO-rich phase. For *stretched* and *in-situ stretched* samples with relatively long PTMO block lengths, an additional resonance with different chemical shifts for the OCH_2 carbons of PTMO and with a restricted mobility was observed. This new resonance, which is also found in *unstretched* samples at temperatures of −30 °C, is assigned to strain-induced crystalline PTMO. The amount of crystalline PTMO increases linearly with the sample strain. It appears that, in *stretched* samples, heating to 50 °C leads to irreversible melting of the PTMO crystals, in contrary to the *in-situ stretched* samples, which show recrystallization upon cooling to room temperature. 2D rotor-synchronized $^{13}C-CPMAS$ experiments revealed a high orientation of the hard and soft phases upon stretching.

I. Introduction

Block copolymers of poly(butylene terephthalate) (PBT) and poly(tetramethylene oxide) (PTMO) are poly(ether esters), which belong to the class of thermoplastic elastomers. They consist of hard segments formed by the PBT blocks and soft segments consisting of PTMO chains.

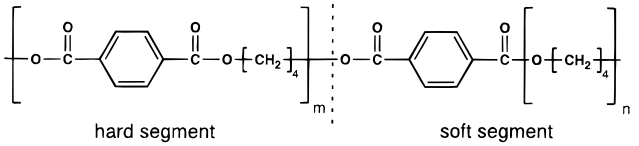

As in the case of several other thermoplastic elastomers such as poly(styrene-*b*-butadiene-*b*-styrene) or polyurethanes, also in poly(ether esters) the hard segments tend to form rigid (in our case semicrystalline) domains which are embedded in an amorphous, rubbery matrix.[1] This microphase structure of hard and soft segments is strongly responsible for the mechanical properties of the copolymer system. Similar to the chemical cross-links (sulfur bonds) in vulcanized rubber, the crystalline hard-segment domains of the thermoplastic elastomers act as physical cross-links and thus cause the elastomeric nature of the material. Compared to the conventional rubbers, thermoplastic elastomers are superior in processing and recycling.

The PBT/PTMO block copolymers are of special interest due to their excellent mechanical properties, like mechanical strength and elastic properties in a wide temperature range. The positive characteristics of both the homopolymers are combined, i.e., a high melting point (PBT) and a low T_g (PTMO). By varying the amount and block length of the hard and soft segments, a wide range of materials with different mechanical properties can be covered.

For elastomeric materials it is of special interest to study the changes in microphase structure that occur in the material during mechanical deformation. Knowledge of the microphase behavior and strain-induced chain alignment is essential for a better understanding of the macroscopic properties of these materials. ^{13}C solid-state NMR spectroscopy is a well-established tool for investigation of the microphase structure of polymers. To study the effect of mechanical deformation, we performed NMR experiments on (i) *unstretched* materials, (ii) *stretched* materials allowed to relax prior to NMR experiments, and (iii) stretched materials under tension with constant strain (*in-situ stretched*). To perform the last type of NMR experiments, a special method was developed to keep the *in-situ stretched* samples in the MAS rotor at constant strain and under tension. A similar approach has also been used by other groups studying in-situ stretched rubbers by static NMR methods[2] and investigating in-situ stretched fibers by $^{13}C-CPMAS$.[3,4] We completed the set of methods by providing a technique to measure bulk in-situ stretched elastomers by MAS NMR spectroscopy. Various $^{13}C-CPMAS$ experiments, including carbon-$T_{1\rho}$ and proton-$T_{1\rho}$ relaxation experiments, variable contact time measurements, 2D rotor-synchronized $^{13}C-CPMAS$ experiments (determination of molecular orientation), have been performed to study the microphase structure

S0024-9297(97)01467-8 CCC: $15.00
Published on Web 02/11/1998

Table 1. Composition of the PBT/PTMO Block Copolymers

sample	amount of PTMO (wt %)	block length PTMO (g/mol)	$\bar{P}_n$(PTMO)	$\bar{P}_n$(PBT)
A2000/60	60	2000	27.7	6.5
A1500/60	60	1500	20.8	5.0
A1000/60	60	1000	13.9	3.5
A1500/50	50	1500	20.8	7.5
A1000/50	50	1000	13.9	5.2
A1000/35	35	1000	13.9	9.7

[a] $\bar{P}_n$ = number average degree of polymerization.

of PBT/PTMO block copolymers and changes on the molecular level upon stretching.

II. Experimental Section

Samples. We investigated a series of six PBT/PTMO block copolymers, differing in the amount and block length of PTMO, which were prepared at DSM Research B.V., Galeen, The Netherlands. The block lengths and compositions of the samples are given in Table 1. The molecular weight M_n of all samples is approximately 25 000. The M_w/M_n ratio for PTMO and PBT is about 1.6 and 2, respectively. The PBT block length is determined by the hard/soft ratio and the PTMO block length. The samples designation A*x*/*y* is given according to the PTMO block length (*x* in g/mol) and the PTMO content (*y* in wt%). For stretched samples the extensions -b, -s, and -i are used to indicate *stretched to break*, *stretched*, and *in-situ stretched* samples, respectively. All samples were injection-molded either into the form of test bars or into plates.

Sample Preparation for NMR Experiments

(i) Unstretched Samples. For the NMR measurements of the *unstretched* samples, 4 × 4 × 10 mm blocks were cut from the test bars and loaded into a 7 mm ZrO_2 MAS rotor. To allow stable rotation, the empty spaces in the rotor were filled with talcum powder.

(ii) Stretched Samples. The *stretched* samples first were stretched to a certain strain or until break using a tensile tester (Schenk−Trebel) and then were taken out of the machine and relaxed to a stress of zero. Since the samples deform plastically in the range of loads studied ($\epsilon > 50\%$),[5] incomplete elastic recovery was observed. The percentage rest strain was determined to be analogous to the strain by

$$\epsilon_{rest} = \frac{l - l_0}{l_0} \times 100$$

where l_0 is the initial length of the test bar and l the length after stretching and stress relaxation for at least 12 h (l_0 and l were measured between ink marks on the tensile bar in the proximity of the clamps).

A series of six samples was stretched to break. For preparation of these samples we used test bars with a starting cross section of 10 × 4 mm. After stretching to break, the samples had thinned to a width of 4−5 mm and a thickness of approximately 2 mm. Two strips with a length of 10 mm each were cut out from the samples in the direct neighborhood of the breaking point. These strips were then stacked into the 7 mm ZrO_2 MAS rotor with the stretching direction parallel to the rotor axis and the empty spaces filled with talcum powder. For the 2D rotor-synchronized $^{13}C-CPMAS$ measurements, two rhombic pieces were cut out and stacked into the rotor so that the angle between the stretching direction and the rotor axis was 60°. We chose a 60° angle, since this angle gives a relatively large number of experimental spinning sidebands in the 2D spectrum.[6]

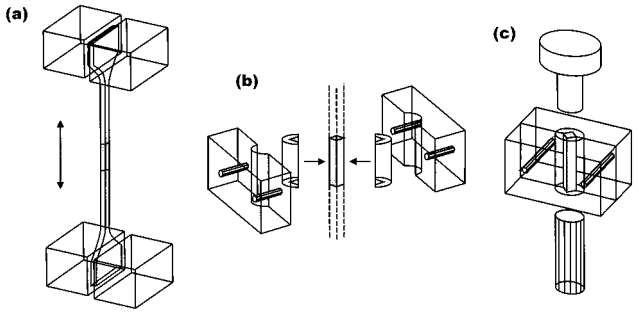

Figure 1. Preparation of *in-situ stretched* samples.

Table 2. Characteristic Stretching Data of the Three *In-situ Stretched* PBT/PTMO Samples of A2000/60, and Their *Stretched* Reference Samples

sample	tensile force F (N)	tensile stress σ (MPa)	tensile strain ϵ (%)	rest strain ϵ_{rest} (%)
A2000/60-Ii (*in-situ stretched*)	125	7.8	160	160
A2000/60-Is (*stretched*)	125	7.8	160	30
A2000/60-IIi (*in-situ stretched*)	185	11.6	354	354
A2000/60-IIs (*stretched*)	185	11.6	354	126
A2000/60-IIIi (*in-situ stretched*)	325	20.3	709	709
A2000/60-IIIs (*stretched*)	325	20.3	709	373

For one sample (A2000/60) we prepared three additional samples stretched to different strains (A2000/60-Is, A2000/60-IIs, A2000/60-IIIs), which serve as a reference for the *in-situ stretched* samples (see Table 2). Here, test bars with a symmetrical starting cross section (4 × 4 mm) were used. After stretching, the sample was immediately taken out of the stretching machine and was allowed to relax to a constant rest strain for approximately 24 h. Then a piece of 10 mm length was cut out from the middle of the test bar and placed in the rotor with the stretching direction parallel to the rotor axis. To allow stable rotation, the samples were kept in the middle of the rotor by wrapping them up with Teflon tape.

(iii) In-Situ Stretched Samples. Samples that were kept under tension in the MAS rotor with a constant strain are called *in-situ stretched*. The preparation method for those samples is schematically illustrated in Figure 1. For the preparation of *in-situ stretched* samples test bars with a square starting cross section of 4 × 4 mm are stretched by the tensile tester to a prescribed strain ϵ. Then stress relaxation to a constant value (stress > 0) is allowed by leaving the samples in the tensile tester at ϵ for approximately 12 h (Figure 1a). Next, two half-cylinders made from Kel-F with a centric square hole are adjusted to the middle of the sample, so that the *in-situ stretched* sample fits to this square hole. This fitting procedure is essential for the sample preparation. To minimize the error, the stretching machine was stopped at the point where the half-cylinders just came into contact when putting them around the cross section of the samples. Since the cross section hardly changed during the next 12 h of stress relaxation (probably because the flow of material into the center compensates for the shrinkage of the material during crystallization), the half-cylinders still almost

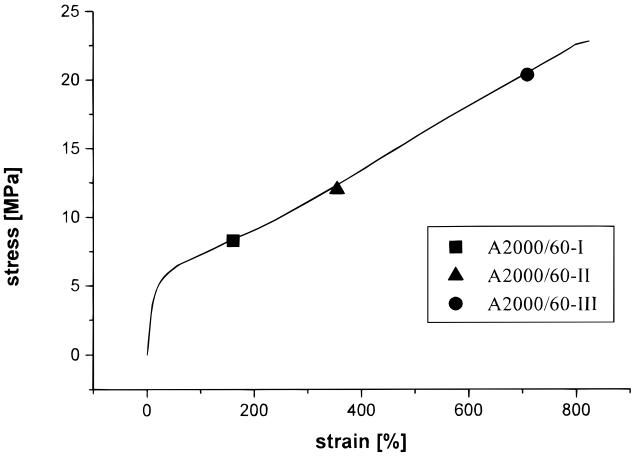

Figure 2. Stress−strain diagram of sample A2000/60. The maximum stresses and strains of the three *in-situ stretched* samples and their *stretched* reference samples are marked.

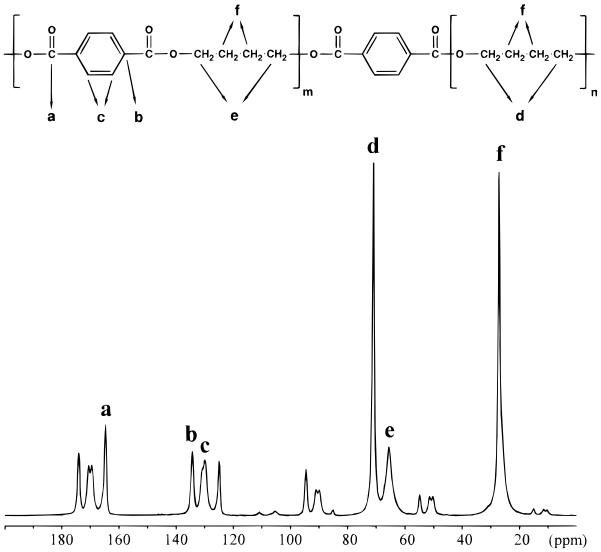

Figure 3. Assignment of the resonances of the ^{13}C−CPMAS spectrum of the *unstretched* sample A2000/60. All resonances not marked by a letter are spinning sidebands. Note that the OCH_2 carbons of the first tetramethylene oxide unit directly connected to the terephthalate group belong to resonance e and not to resonance d.

perfectly fitted to the in-situ stretched sample. The Kel-F half-cylinders are then clamped using two metal blocks with a cylindrical hole (same diameter as the Kel-F cylinder). Next, the sample is cut above and below the cylinder. Hence, that part of the sample being inside the Kel-F half-cylinders is mechanically kept under uniaxial tension at the fixed strain ϵ, since the sample has no space to contract. Here we can neglect the shrinkage of the material, which is caused by density changes during crystallization, since we assume that the main crystallization process takes place during the first 12 h, before the sample is clamped and cut (Figure 1b). In the last step, the two Kel-F half-cylinders with the *in-situ stretched* sample in between are pressed into a 7 mm ZrO_2 MAS rotor whose inner diameter has exactly the same size as the outer diameter of the Kel-F cylinder (Figure 1c).

For sample A2000/60 we prepared three *in-situ stretched* samples with different strains (A2000/60-Ii, A2000/60-IIi, A2000/60-IIIi), of which the characteristic data are shown in Table 2. The tensile stresses and strains of the samples are also visualized by the stress−strain curve of sample A2000/60 shown in Figure 2.

NMR. All NMR measurements were performed on a Bruker ASX-400 spectrometer operating at a frequency of 400 MHz for protons. A double-bearing CPMAS probe was used with 7 mm ZrO_2 rotors. The spinning speed in all experiments was 4 kHz. For all cross polarization experiments the 90° pulse length on protons and carbons was 6 μs, the cross-polarization time was 1 ms, and the recycle delay was 2 s. Acquisition of the carbon signal was always performed under proton decoupling with a proton decoupling field of 41.7 kHz. Adamantane was used to optimize the Hartmann−Hahn condition, and it also served as an external secondary chemical shift reference (38.56 ppm for the methylene resonance relative to TMS). The ^{13}C−MAS experiment with direct excitation has been recorded using a recycle delay of 25 s to ensure full relaxation of all carbon spins. For all NMR relaxation experiments spectra at different delay times were obtained by block averaging to avoid possible effects of spectrometer drifts.

The T_{CH} time constants were determined using the standard CP pulse sequence with variable contact time (10 μs to 10 ms). The peak intensities as a function of the contact time τ were fitted to either a monoexponential or a biexponential function of the type[7]

$$I(\tau) = \sum_i I_{0i} \frac{\exp\left(-\frac{\tau}{T_{1\rho}^{H}}\right) - \exp\left(-\frac{\tau}{T_{CHi}}\right)}{\left(1 - \frac{T_{CHi}}{T_{1\rho}^{H}}\right)} \qquad (1)$$

For the proton-$T_{1\rho}$ experiment a variable spin-lock period (0.1 −23 ms) on protons was used and the decay of proton magnetization was monitored via the carbon spins using cross polarization. For the carbon-$T_{1\rho}$ measurement the cross-polarization period was followed by a variable spin-lock pulse (0.1−30 ms) on carbons. The integral line intensities as a function of the variable spin-lock time τ were fitted to either a mono- or biexponential decay function

$$I(\tau) = \sum_i I_{0i} \exp\left(-\frac{\tau}{T_{1\rho i}^{H/C}}\right) \qquad (2)$$

The 2D rotor-synchronized ^{13}C−CPMAS experiment was performed using the pulse sequence designed by Harbison et al.[8] The down edge of the rotor signal triggers the start of the pulse sequence. After a constant waiting time of 10 μs, the evolution time t_1 was incremented in 15 steps of $^1/_{16}$ of the rotor period, yielding 16 FIDs.

III. Results and Discussion

^{13}C−CPMAS Spectrum. Figure 3 shows a ^{13}C−CPMAS spectrum of the *unstretched* sample A2000/60. In addition to the spinning sidebands, we can observe six resonances (a−f) which are assigned to the structural units as shown in Figure 3.[9] The spectrum shows four PBT resonances, the carbonyl carbons (164.7 ppm), the nonprotonated aromatic carbons (134.4 ppm), the protonated aromatic carbons (131.0 ppm/129.8 ppm), and the OCH_2 groups of PBT (65.7 ppm). For PTMO a resonance for the OCH_2 groups at 71.2 ppm is observed.

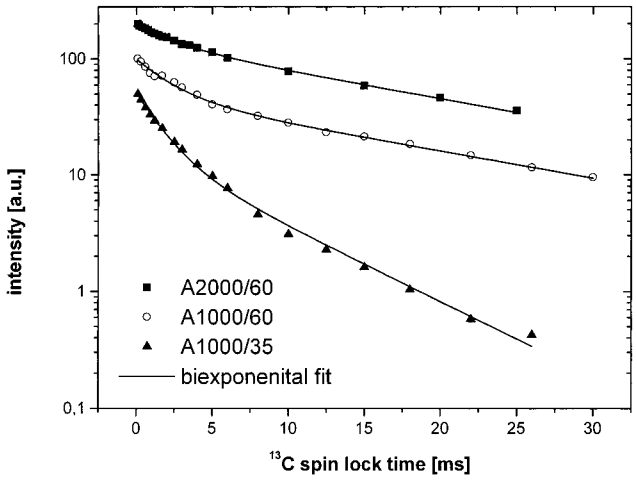

Figure 4. Carbon-$T_{1\rho}$ decay of the OCH_2(PTMO) carbons of the unstretched samples A2000/60, A1000/60, and A1000/35. The solid lines represent least-squares fits of the experimental data using the biexponential function given in eq 2.

Table 3. Proton-$T_{1\rho}$, Carbon-$T_{1\rho}$ and T_{CH} Times of the OCH_2(PTMO) Resonance of the *Unstretched* Samples A2000/60, A1000/60, and A1000/35[a]

	room temperature			
	A2000/60	A1000/60	A1000/35	70 °C A2000/60
^{1}H-$T_{1\rho}$ (ms)	1.9 (39)	2.1 (45)	1.9	2.2 (21)
	11 (61)	6.8 (55)		23 (79)
^{13}C-$T_{1\rho}$ (ms)	2.5 (32)	2.3 (53)	1.7 (71)	9.2 (51)
	18 (68)	18 (47)	6.9 (29)	60 (49)
T_{CH} (μs)	75 (30)	51 (42)	48 (62)	
	2300[b] (70)	1400[b] (58)	530[b] (38)	

[a] The relative fraction of the relaxation component (%) is given in parentheses. The experimental error is approximately 10%.[b] The experimental error for these values is about 30%, due to oscillations in the cross polarization curve, which are common for very mobile systems.[12−14]

It should be noted that the OCH_2 carbons of the first PTMO unit which is directly connected to the terephthalate group do not contribute to resonance d at 71.2 ppm but to resonance e at 65.7 ppm. The internal methylene groups of both hard and soft segments give rise to a peak at 27.5 ppm with an upfield shoulder. Since the OCH_2 carbons of PBT and PTMO have different chemical shifts, it is possible to investigate the hard and soft segments separately. This study concentrates on the soft phase, for which the OCH_2 resonance of PTMO is used.

(a) Unstretched Samples. Molecular Scale Miscibility. To study the molecular scale miscibility of PBT/PTMO block copolymers, several relaxation time experiments on different *unstretched* PBT/PTMO samples were performed. In all relaxation time measurements, the OCH_2 resonance of PTMO shows a biexponential behavior (except for ^{1}H−$T_{1\rho}$ of sample A1000/35 which is explained later). This strongly suggests that two different types of PTMO units are present in all investigated samples. As an example the decay of magnetization of the OCH_2(PTMO) carbons in a ^{13}C−$T_{1\rho}$ experiment for *unstretched* samples A2000/60, A1000/60, and A1000/35 is given in Figure 4. In Table 3 the proton-$T_{1\rho}$, carbon-$T_{1\rho}$ and the T_{CH} times of the OCH_2-(PTMO) resonance of *unstretched* samples A2000/60, A1000/60, and A1000/35 are listed. This heterogeneous character of PTMO is also found by inversion−recovery cross-polarization experiments,[10] which clearly show two

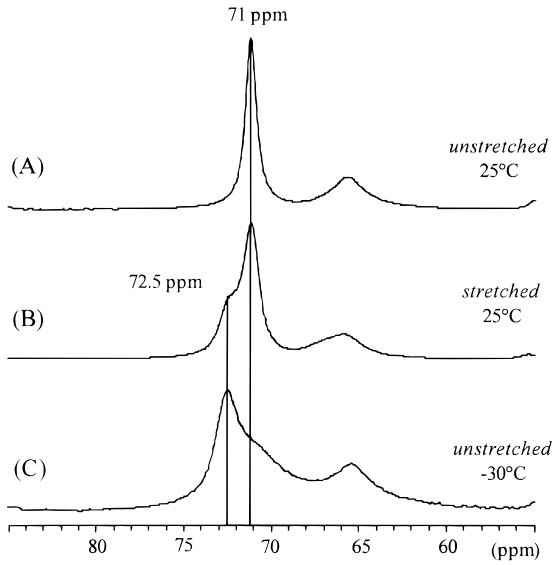

Figure 5. ^{13}C−CPMAS spectrum showing the OCH_2 groups of the *unstretched* sample A2000/60 at 25 °C (A), the *stretched* (to break) sample A2000/60-b at 25 °C (B), and the *unstretched* sample A2000/60 at −30 °C (C).

OCH_2(PTMO) resonances with different line widths inverting at different delay times.[11]

In the case of the very mobile carbons the dipolar coupling of carbon spins to the surrounding protons is weaker than that of more rigid carbons and therefore cross polarization is less efficient, resulting in a longer T_{CH} time. Regarding the variable contact time measurements, we can therefore clearly assign the long T_{CH} times to relatively mobile OCH_2 carbons, while the short T_{CH} times belong to OCH_2 carbons with restricted mobility. For the assignment of the $T_{1\rho}$ times the relative fractions of carbons with long and short relaxation times can be considered. Although this ratio is not completely quantitative, a comparison of the ratios for the T_{CH} measurements with the ratios found in the $T_{1\rho}$ experiments suggests that the long $T_{1\rho}$ times can be assigned to the more mobile carbons while the short $T_{1\rho}$ times belong to the carbons with restricted mobility. This assignment is supported by a proton-$T_{1\rho}$ and a carbon-$T_{1\rho}$ measurement of sample A2000/60 at 70 °C (see Table 3). The long $T_{1\rho}$ time constants increase with increasing temperature, which is typical for highly mobile systems.

We assign the more mobile carbons to PTMO-rich domains and the less mobile carbons to mixed PBT/PTMO domains (possibly the PBT/PTMO interphase), where the mobility of the PTMO is restricted by the presence of PBT segments. The influence of the PTMO block length and the PTMO content on the fractions of the PTMO-rich phase and the mixed PBT/PTMO phase in all relaxation time measurements supports this assignment (Table 3). As expected, the fraction of PTMO-rich domains decreases by decreasing the PTMO block length (compare A2000/60 and 1000/60) and by decreasing the total amount of PTMO in the sample (compare A1000/60 and A1000/35).

Regarding the proton-$T_{1\rho}$ data, we observe a biexponential behavior for samples A2000/60 and A1000/60, whereas the magnetization decay for sample A1000/35 can be fitted monoexponentially. Since the ^{1}H−$T_{1\rho}$ times of samples A2000/60 and A1000/60 are not averaged by spin diffusion, we can assume that the PTMO-rich and mixed PBT/PTMO domains in these samples

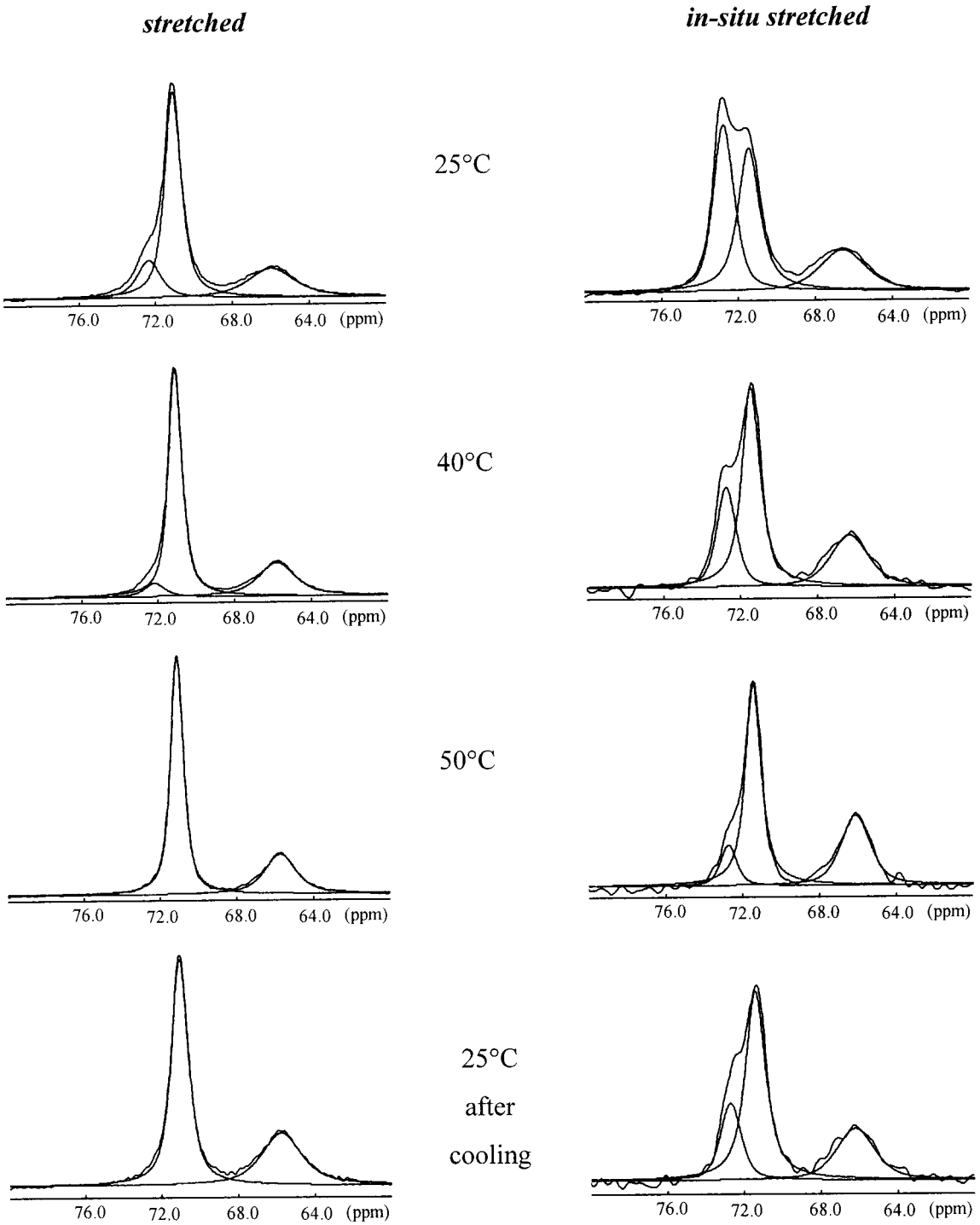

Figure 6. $^{13}C-CPMAS$ spectra at different temperatures for the *stretched* sample A2000/60-b (left) and the *in-situ stretched* sample A2000/60-IIIi (right). All experiments were performed while the samples remained in the rotor. For the in-situ stretched samples this implies that during the temperature treatment the sample remained under stress. Between temperature changes the system was given 15 min to adapt. After recording the spectrum at 50 °C, the sample was allowed to cool for 1 h, before taking the last room temperature spectrum.

have at least a dimension of 1 nm. In sample A1000/35, where T_{CH} and $^{13}C-T_{1\rho}$ point to the existence of two soft phases with different mobilities, spin diffusion is effective, resulting in a single $^{1}H-T_{1\rho}$ value, which indicates that here the dimensions of both phases are much smaller, as expected for a sample with short PTMO block length and low PTMO content. Our results are in agreement with DMA measurements.[5] For the samples A2000/60 and A1000/60 two T_g's were found at −70/−20 and −65/−35 °C, respectively, indicating the existence of two separated amorphous phases with different compositions. Sample A1000/35 showed only one broad T_g at −42 °C, which means that the mobile and rigid PTMO in this case are not well separated as was also found in the $^{1}H-T_{1\rho}$ experiment.

(b) Stretched and In-Situ Stretched Samples. Strain Induced Crystallization of PTMO. With the information about the microstructure of the soft phase of PBT/PTMO block copolymers obtained by investigating the *unstretched* samples, we now study the changes

Table 4. Fractions of Crystalline PTMO as Determined by Deconvolution of the $^{13}C-CPMAS$ Spectra of Samples A2000/60-b (*Stretched* to Break) and A2000/60-IIIi (*In-Situ Stretched*), Recorded at Different Temperatures[a]

	amount of crystalline PTMO (%)	
temperature (°C)	A2000/60-b	A2000/60-IIIi
25	6	26
40	2	14
50	0	6
25 (after cooling)	0	11

[a] The fractions are corrected for difference in CP efficiency.[20] The error caused by deconvolution on the corrected fractions is approximately 1%.

in microstructure that occur upon stretching. In Figure 5 an enlarged part of the $^{13}C-CPMAS$ spectrum showing the OCH_2 resonance of the *unstretched* sample A2000/60 (A) and the corresponding *stretched* sample A2000/60-b (B) is displayed. When we compare spectra A and B, the most obvious change is the appearance of a new resonance for the OCH_2 carbons of PTMO shifted downfield by approximately 1.3−1.4 ppm. This new PTMO resonance is also observed by cooling an *unstretched* sample to −30 °C, as can be seen in Figure 5C. WAXS and DSC measurements[5] show that the PTMO segments of A2000/60 crystallize at temperatures near $T = -30$ °C. Therefore, we ascribe this new resonance at 72.5 ppm appearing in the *stretched* and also in *in-situ stretched* A2000/60 samples to strain-induced crystallization of PTMO segments. The ability of PTMO to crystallize under strain was also found by Tashiro et al.[15] using IR spectroscopy.

All our NMR results are in agreement with this assignment: (i) It is known that PTMO crystallizes in an all-trans conformation of the methylene carbons.[16] We assigned the new resonance at 72.5 ppm to all-trans OCH_2 groups and the 71 ppm resonance to OCH_2 groups which can perform trans−gauche transitions in the methylene chain very rapidly (γ-gauche effect[17]), which is in agreement with an assignment for the OCH_2 resonances of PTMO homopolymers or phthalic ester terminated PTMO oligomers.[16,18] (ii) In experiments with short contact time and in IRCP experiments[11] the new resonance shows short T_{CH} times. This means that the carbons responsible for the 72.5 ppm resonance are in a rigid environment, as can be expected for crystalline PTMO. (iii) The 2D rotor-synchonized $^{13}C-CPMAS$ experiment showed that the carbons resonating at 72.5 ppm are highly oriented (see below).

Temperature Dependence of the Strain-Induced Crystallization. Figure 6 shows the $^{13}C-CPMAS$ spectra of the *stretched* A2000/60-b sample (stretched to break) and the *in-situ stretched* sample A2000/60-IIIi at 25,40, and 50 °C as well as the spectrum recorded immediately after cooling the samples back to room temperature. The fractions of crystalline PTMO as determined by deconvolution[19] of the OCH_2(PTMO) resonance in the CP spectra (corrected for CP enhancement[20]) of samples A2000/60-b and A2000/60-IIIi are given in Table 4. For both samples the amount of crystalline PTMO decreases with increasing temperature. After heating to 50 °C crystalline PTMO totally disappears for the *stretched* sample and does not recover after cooling. This effect is ascribed to melting of the strain-induced PTMO crystals. The NMR results are in agreement with DSC measurements performed on *stretched* samples A2000/60, in which a melting peak at approximately 45 °C was found in the first heating.[5]

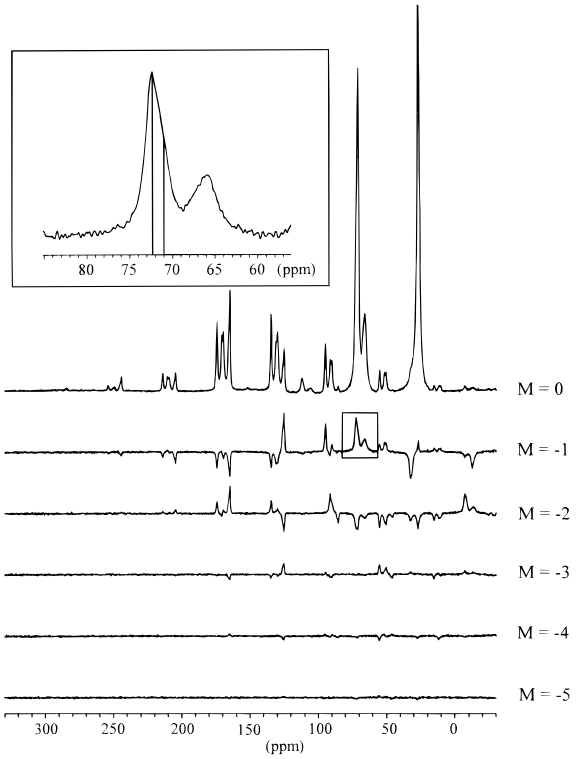

Figure 7. Stack plot of the negative *M* slices of the 2D rotor-synchronized $^{13}C-CPMAS$ experiment for the *stretched* sample A2000/60-b. The inset shows that the 72.5 and 71 ppm resonances are oriented.

Since 50 °C is close to the T_g of pure PBT, it is suggested that the deformed PBT domains in the *stretched* samples keep the PTMO chains under strain at room temperature. Heating to 50 °C results in an increase of mobility of the amorphous PBT segments, which causes a loss of internal strains in PTMO domains and hence a destruction of the strain-induced PTMO crystals.

In contrast to the *stretched* sample for the *in-situ stretched* sample at 50 °C, there is still some crystalline PTMO left, and after cooling the sample down to room temperature, the amount of the crystalline PTMO resonance increases again, however, to a value lower than the initial value. Apparently, in the *in-situ stretched* sample not all crystalline PTMO is melted, and after cooling the sample to room temperature again, a recrystallization takes place. This suggests that in the case of the *in-situ stretched* sample heating to 50 °C also leads to a greater mobility of the PBT segments and therefore a reduction of the internal strain on PTMO, which results in a decrease of crystalline PTMO. However, since the external force is still present after cooling in the *in-situ stretched* sample, the PTMO segments can recrystallize. It is likely that heating causes a partial loss in strain on some domains of the *in-situ stretched* sample, which can explain that the original amount of crystalline PTMO cannot be reached again after cooling the *in-situ stretched* sample to room temperature.

Strain-Induced Orientation. To study the orientation of PBT and PTMO domains after stretching, we performed a 2D rotor-synchronized $^{13}C-CPMAS$ experiment[8] on the *stretched* (to break) sample A2000/60-b.[21] As a reference the experiment was also performed on the *unstretched* sample A2000/60. In this type of 2D spectrum the "normal" CPMAS spectrum is obtained in the ω_2 dimension, whereas in the ω_1 dimension a spinning sideband pattern appears which is character-

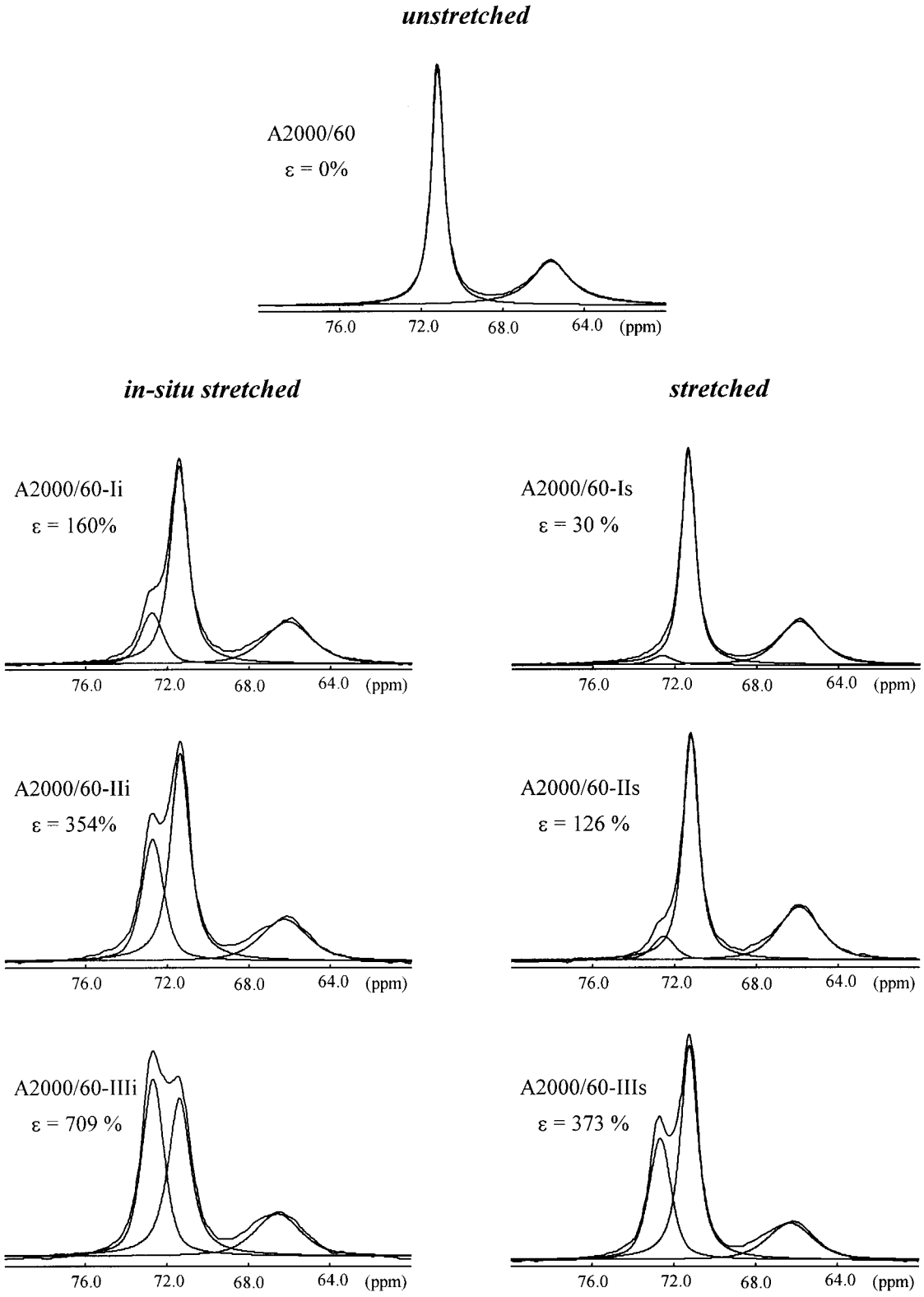

Figure 8. $^{13}C-CPMAS$ spectra of the *unstretched*, the *in-situ stretched*, and the *stretched* samples at different strains/rest strains for sample A2000/60.

istic of the degree of order in the sample. If the investigated sample is not oriented along a preferential order axis, only intensities in the $M = 0$ slice are obtained. The higher the orientation of the sample, the more sideband intensities in higher M slices are obtained. As expected, the *unstretched* sample does not show sideband intensities in the ω_1 dimension, which means that no orientation is caused by injection-molding of the samples. In Figure 7 the $M = 0$ and the negative M slices of the 2D spectrum for the *stretched* sample A2000/60-b are shown in the form of a stack plot. From these spectra we see that the PBT and the PTMO units are oriented after stretching. An evaluation of the spinning sideband pattern for PBT yielding quantitative information on the orientation has been performed, and the PBT domains are found to be highly oriented (orientation parameters for the nonprotonated aromatic carbons of PBT: $\langle P_2 \rangle = 0.79$, $\langle P_4 \rangle = 0.52$). The high

Table 5. Fractions of Crystalline PTMO as a Function of Strain or Rest Strain for the *In-Situ Stretched* and *Stretched* Samples of A2000/60 As Determined by Deconvolution of the OCH_2(PTMO) resonance[a]

in-situ stretched A2000/60		*stretched* A2000/60	
strain ϵ (%)	amount of crystalline PTMO (%)	rest strain ϵ_{rest} (%)	amount of crystalline PTMO (%)
160	9	30	2
354	17	126	4
709	26	373	18

[a] The amounts are corrected for the differences in CP efficiency.[20]

orientation suggests that not only the crystalline PBT units but also the amorphous PBT blocks are aligned to the stretching direction. A quantitative analysis of the spinning sideband intensities of the OCH_2(PTMO) resonance was not performed since it would not yield reliable data due to the low number of integratable sideband intensities. However, the spectra qualitatively show the orientation of the PTMO units in the *stretched* samples. Regarding the sideband intensities of the higher *M* slices in detail, it appears that both the crystalline (72.5 ppm) and the amorphous OCH_2 groups of PTMO (71 ppm) are oriented. The 2D intensities of the 71 ppm resonance are less intense compared to the 72.5 ppm resonance, indicating that the noncrystalline PTMO chains are less oriented than the crystalline. This can be expected, since in the noncrystalline PTMO phases, which are above their T_g at room temperature, the mobility of the PTMO chains is relatively high, leading to a fast decrease of strain-induced order.

Dependence of Crystalline PTMO on the Strain. To obtain more quantitative information on the strain-induced PTMO crystallization, we investigated *in-situ stretched* and *stretched* samples at different strains. Figure 8 shows the OCH_2 resonances of the $^{13}C-$CPMAS spectra of the *unstretched* sample A2000/60, the three *in-situ stretched* samples A2000/60-Ii, A2000/60-IIi, and A2000/60-IIIi, and their corresponding *stretched* samples A2000/60-Is, A2000/60-IIs, and A2000/60-IIIs. The fraction of crystalline PTMO appears to be strongly dependent on the strain. It increases with increasing strain in the series of *in-situ stretched* samples or increasing rest strain in the series of *stretched* samples. The *in-situ stretched* samples, however, always show a greater fraction of crystalline PTMO phase compared to their corresponding *stretched* reference samples, which were allowed to relax to a constant, smaller rest strain. The fractions of crystalline PTMO corrected for CP enhancement[20] as determined by deconvolution[19] are given in Table 5. In Figure 9 the percentage amount of the crystalline PTMO resonance at 72.5 ppm is plotted against the fixed strain for the *in-situ stretched* samples and against the rest strain after relaxation for a number of *stretched* samples. The amount of crystalline PTMO grows almost linearly with the strain or the rest strain, respectively. From the plot it is obvious that the *stretched* and the *in-situ stretched* samples show the same dependence on ϵ. This means that, e.g., a sample stretched to a maximum strain of ca. 700% and relaxed to a rest strain of ca. 350% with a zero stress shows the same amount of crystalline PTMO as a sample stretched to a strain of 350% and kept under tension at this constant strain.

Dependence of the Strain-Induced Crystallization on the PTMO Block Length and Content. To

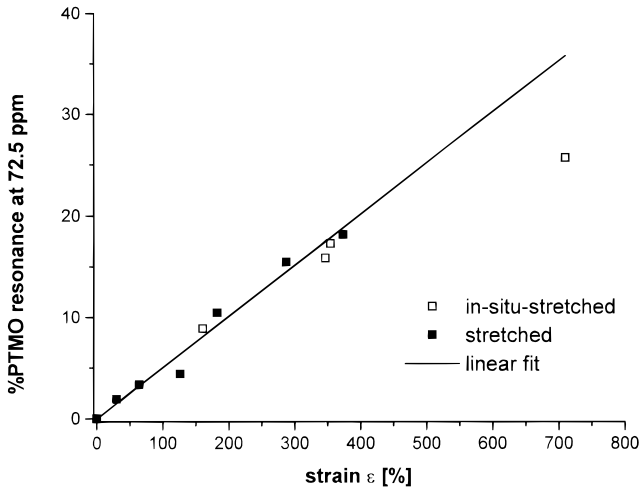

Figure 9. Fraction of the 72.5 ppm resonance relative to the total intensity of the OCH_2(PTMO) resonance as a function of the strain for the *in-situ stretched* samples and the rest strain for the *stretched* samples of A2000/60. Except for the sample with highest strain, the data can be fitted linearly.

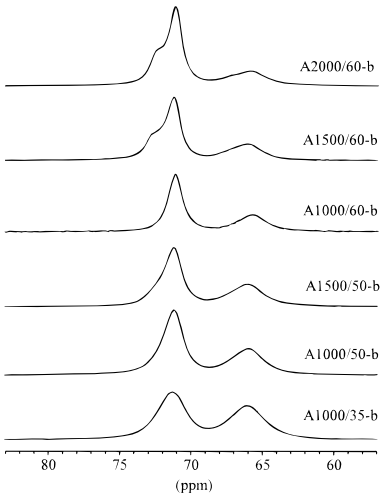

Figure 10. $^{13}C-$CPMAS spectra of PBT/PTMO samples with different PTMO block lengths and PTMO contents. All samples have been stretched to break.

determine the influence of PTMO block length and PTMO content on the strain-induced PTMO crystallization, $^{13}C-$CPMAS experiments were performed on six different PBT/PTMO block copolymers, which were all *stretched* to break. The corresponding spectra are shown in Figure 10. Only samples A2000/60-b and A1500/60-b show a clear shoulder at 72.5 ppm for the OCH_2(PTMO) resonance, for sample A1500/50-b an unsymmetrical OCH_2(PTMO) peak can be observed, and the *stretched* samples A1000/60-b, A1000/50-b, and A1000/35-b show no additional resonance upon stretching. This means that the ability to form crystalline PTMO phases upon stretching that are stable at room temperature after stress relaxation increases with increasing PTMO block length and increasing PTMO content. This is consistent with earlier results (see unstretched samples), which show a high fraction of the highly mobile PTMO-rich domains in samples with long PTMO block length and high PTMO content. Therefore, it is likely that the crystalline domains will predominantly form due to the highly mobile PTMO-rich domains.

IV. Conclusions

By application of several NMR relaxation time measurements on the *unstretched* PBT/PTMO block copolymer system, we found that the amorphous phase is microphase-separated into a mobile PTMO-rich phase and a PBT/PTMO mixed phase with restricted mobility. This microphase separation is most pronounced in samples with long PTMO block length and high PTMO content.

To study the effect of deformation on the microphase structure of these samples, MAS NMR experiments were performed on *stretched* samples that were allowed to relax and on *in-situ stretched* samples. To measure the last type of samples, we developed a new method to keep the sample under tension at constant strain in the spinning rotor. Both types of stretched samples show an additional OCH_2(PTMO) resonance, which is assigned to strain-induced crystallization of PTMO. This resonance is only observed for PBT/PTMO block copolymers with relatively long PTMO block length and high PTMO content. Heating to 50 °C causes the strain-induced PTMO crystals to melt; in the case of *in-situ stretched* samples a recrystallization by cooling back to room temperature is observed. It was shown that the amount of strain-induced crystallization of PTMO shows the same dependence on the strain/rest strain for *in-situ stretched* and *stretched* samples, respectively. The fraction of crystalline PTMO increases almost linearly with increasing strain/rest strain. 2D rotor-synchronized $^{13}C-$CPMAS measurements revealed that after stretching the PBT units as well as the PTMO units are oriented along the stretching direction. For PTMO not only did the strain-induced crystalline PTMO blocks show orientation but also for the amorphous PTMO some orientation was found.

Acknowledgment. We thank DSM Research for kindly providing the samples, for the fruitful discussions, and for the financial support of this work and Dipl.-Ing. M. Zähres for his help during the development of the technique to measure *in-situ stretched* samples.

References and Notes

(1) Holden, G. *Encycl. Polym. Sci. Eng.* **1986**, *5*, 416.
(2) Blümler, P.; Blümich, B. *Acta Polym.* **1993**, *44*, 125.
(3) Shi, J. F.; Dickinson, L. C.; Chien, J. C. W. *Macromolecules* **1992**, *25*, 3278.
(4) Dickinson, L. C.; Shi, J. F.; Chien, J. C. W. *Macromolecules* **1992**, *25*, 1224.
(5) Dijkstra, K.; Martens, H.; Soliman, M.; Borggreve, R., Lecture at the 4th International Symposium on TPE's, Kolobrzeg, 1997.
(6) Gabriëlse, W.; Angad Gaur, H.; Veeman, W. S. *Macromolecules* **1996**, *29*, 9 (11), 4125.
(7) Mehring, M. *High-resolution NMR Spectroscopy in Solids, NMR Basic Principles and Progress*; Springer-Verlag: Berlin, 1976; p 11.
(8) Harbison, G. S.; Vogt, V.; Spiess, H. W. *J. Chem. Phys.* **1987**, *86* (3), 1206.
(9) Jelinski, L. W.; Dumais, J. J.; Engel, A. K. *Macromolecules* **1983**, *16*, 403.
(10) Cory, D. G.; Ritchey, W. M. *Macromolecules* **1989**, *22*, 1611.
(11) Gabriëlse, W., to be published.
(12) Müller, L.; Kumar, A.; Baumann, T.; Ernst, R. R. *Phys. Rev. Lett.* **1974**, *32* (25), 1402.
(13) Demco, D. E.; Tegenfeldt, J.; Waugh, J. S. *Phys. Rev., Part B* **1975**, *11* (11), 4133.
(14) Naito, A.; McDowell, C. A. *J. Chem. Phys.* **1986**, *84* (8), 4181.
(15) Tashiro, K.; Hiramatsu, M.; Ii, T.; Masamichi, K.; Hiroyuki, T. *Sen'i Gakkaishi* **1986**, *42* (11), T597.
(16) Hirai, A.; Horii, F.; Kitamaru, R.; Fatou, J. G.; Bello, A. *Macromolecules* **1990**, *23*, 2913.
(17) Ibbett, R. N. *NMR spectroscopy of polymers;* Blackie Academic and Professional: Glasgow, U.K., 1993.
(18) Lillya, C. P.; Baker, R. J.; Hütte, S.; Winter, H. H.; Lin, Y.-G.; Shi, J.; Dickinson, L. C.; Chien, J. C. W. *Macromolecules* **1992**, *25*, 2076.
(19) Although we are aware that the OCH_2(PTMO) resonance consists of at least three different compounds (two peaks with a chemical shift of 71 ppm[11], we chose a two-component fitting procedure to determine the amount of crystalline PTMO, since the fitting gave very satisfying results and could hardly be improved by a three-component fitting.
(20) To determine quantitatively the fraction of strain-induced crystalline PTMO phase, we have to account for the fact that in CP spectra the rigid phases are enhanced, since their cross polarization is more efficient. Therefore, from comparison of the relative amounts of the 72.5 and 71 ppm resonance of a ^{13}C spectrum recorded with direct excitation and one recorded with cross polarization on the same sample, we determined an enhancement factor (rigid/mobile(direct excitation) = 0.3489 × rigid/mobile(CP)). With the assumption that the cross polarization rate for the 72.5 ppm resonance of the differently stretched samples does not change drastically, we can roughly estimate the fraction of crystalline PTMO phase in the A2000/60 samples.
(21) Orientation measurements on the *in-situ stretched* samples using the 2D rotor-synchronized $^{13}C-$CPMAS experiments cannot be performed, since an angle different from zero between the rotor axis and the stretching direction of the sample is demanded, which is not fulfilled. We therefore developed a method to determine the orientation from the 1D $^{13}C-$CPMAS spinning sidebands which will be reported elsewhere (in preparation). It was found, as expected, that the PBT units in the *in-situ stretched* samples are more oriented than those in the *stretched* samples.

MA9714676